Polymer Chemistry

ROYAL SOCIETY OF CHEMISTRY

PAPER

View Article Online
View Journal | View Issue

Cite this: *Polym. Chem.*, 2025, **16**, 3640

Biobased triblock thermoplastic elastomer with betulin- or carvacryl-methacrylate end-blocks by RAFT polymerization†

Aniello Vittore, [a] Pauline Shamraienko, *[b] Ilka Hermes, [b] Qiong Li, [b] Brigitte Voit [b,c] and Lorella Izzo *[a]

In this work, fully biobased acrylic ABA triblock copolymers were synthesized *via* reversible addition-fragmentation chain-transfer (RAFT) polymerization using VISIOMER® Terra C13 (ET13) as the "soft" midblock and two terpenoid-derived methacrylates, betulin methacrylate (BetuMA) and carvacryl methacrylate (CaMA), as the glassy blocks. An "R-linked" bifunctional chain transfer agent (bis-CTA) enabled the formation of ET13 macro-CTAs with controlled molecular weights and narrow dispersity (M_n = 84–229 kg mol^{-1}, $Đ \approx 1.1$). RAFT homo-polymerizations of BetuMA and CaMA yielded well-defined homopolymers (M_n = 20–33 kg mol^{-1}, $Đ < 1.4$) with selective methacrylate reactivity. Chain extension of ET13 macro-CTAs produced a series of ABA triblocks featuring 8–39 mol% glassy content. GPC confirmed molecular weights in the range M_n = 97–415 kg mol^{-1} ($Đ < 1.7$), while DSC and TGA analyses showed distinct glass transitions for soft block, close to −50 °C, and good thermal stability. AFM evidenced clear microphase separation. Mechanical testing revealed that BetuMA-based copolymers (BEB series) achieved tensile strengths up to 3.9 MPa and elongations up to 760%, outperforming CaMA-based analogs (CEC series: $\sigma \leq 1.2$ MPa, $\varepsilon \leq 710\%$). These results demonstrate the efficacy of RAFT polymerization of terpenoid methacrylates in producing high-performance, sustainable thermoplastic elastomers, offering a viable alternative to petroleum-derived thermoplastic elastomers (TPEs).

Received 30th May 2025,
Accepted 9th July 2025

DOI: 10.1039/d5py00540j

rsc.li/polymers

Introduction

Among thermoplastic elastomers (TPEs), styrenic block copolymers (SBCs), like poly(styrene-butadiene-styrene) (SBS) and poly(styrene-isoprene-styrene) (SIS), are widely used but face challenges such as oxidation and UV degradation due to unsaturated bonds in their soft blocks.[1] In this framework, acrylic-based copolymers represent a promising alternative overcoming degradation stability and with advantages like excellent performance as pressure-sensitive adhesives. Commercially available acrylic TPEs are ABA triblock copolymers based on oil-derivatives, with a soft-middle part made of poly(butyl acrylate) and the external glassy blocks of poly(methyl methacrylate)s.[2] In the pursuit of more sustainable materials, considerable efforts are being dedicated to substituting oil-derived components with biobased feedstocks.[3–5] To this end, fatty acid derivatives (*e.g.* poly(lauryl methacrylate)[6,7]) as well as sugar or lignin derivatives (*e.g.* isosorbide,[8] itaconic acid imides,[9] rosin[10]) were investigated as acrylic monomers for the soft or glassy blocks, respectively. Acrylic biobased monomers offer a wide range of possibility to find a balance between sustainability and performance for diverse applications.[11] However, the final copolymers generally exhibit lower performance compared to fossil-based acrylic materials and further investigation appears worthy.

In this work, Reversible Addition Fragmentation Chain Transfer (RAFT), a reversible-deactivation radical polymerization (RDRP), was applied for the synthesis of the ABA triblock copolymers using acrylic monomers from renewable feedstocks. Aiming to evaluate different external blocks while keeping the same middle chain, the following research was conducted using a commercially available biobased monomer for the middle block and two different monomers as the glassy components. Plant oils and their fatty acids, due to their low toxicity, availability, and relatively low price, are a particularly attractive building block sources.[12] A methacrylate alcohol

[a]*Dipartimento di Biotecnologie e Scienze della Vita, Università degli Studi dell'Insubria, via J.H. Dunant 3, 21100 Varese, Italy.*
E-mail: lorella.izzo@uninsubria.it
[b]*Leibniz-Institut für Polymerforschung Dresden e.V., 01069 Dresden, Germany.*
E-mail: shamraienko@ipfdd.de
[c]*Organic Chemistry of Polymers, TUD Dresden University of Technology, 01062 Dresden, Germany*

†Electronic supplementary information (ESI) available: Experimental, spectroscopic and characterisation details. See DOI: https://doi.org/10.1039/d5py00540j

mixture of average C13 is produced by Evonik, under the name VISIOMER® Terra C13-MA (ET13), with 76% of certified biocontent. The relative polymer has a low glass transition temperature (T_g = *ca.* −50 °C), resulting in a promising soft-middle block. It is worth noting that the ET13 structure is very similar to that of lauryl methacrylate, in which the alkyl side chain consists of twelve carbon atoms, already reported as a middle elastomeric block.[6,7,13] ET13 has been used by Milan Marić's research group as a soft polymer to produce sustainable statistical and block copolymers.[14] They also report examples of triblock structures yet with few characterization details, since their work focuses more on the synthesis.[15]

As biobased monomers for the external blocks A, carvacryl methacrylate (CaMA) and betulin methacrylate (BetuMA) were selected. Carvacrol is a monoterpenoid phenol derivable from the essential oil of *Origanum vulgare*,[16] while betulin is a triterpenoid, with a pentacyclic ring structure and three potential reactive sites. Betulin is found in large quantities in the bark of white birch (*Betula papyrifera*).[17] Materials like branches, bark, leaves, and roots are often waste materials from the wood industry and discarded or incinerated, despite containing valuable elements such as lignin and betulin.

Before the copolymer synthesis, the investigation of homopolymers was conducted by their synthesis and characterization. Two series of ABA copolymers incorporating betulin or carvacrol derivatives were synthesized and characterized employing chemical and material analyses.

Experimental

Materials and methods

All chemicals were of reagent grade and used as received unless otherwise indicated. VISIOMER Terra C13-MA (ET13, Evonik) was passed through a column of basic alumina to remove inhibitors prior to use. *S*-4-Cyano-4-(dodecylthiocarbonothioylthio)pentanoic acid (CDP) was purchased from Agene Chemicals. Azobisisobutyronitrile (AIBN, Merck, 98%) was recrystallized from methanol and dried in vacuum prior to use. Betulin (Betu, 98.3%) was supplied biobased from Nature Science Technologies chemicals and dried under vacuum at 40 °C overnight before usage. Toluene, 1,4-dioxane, dichloromethane (DCM), anhydrous magnesium sulfate ($MgSO_4$) and 1,4-butanediol were purchased from Merck. 4-Dimethylaminopyridine (DMAP), dicyclohexyl carbodiimide, methacrylic anhydride, 1,3,5-trimethylbenzene and carvacrol (>98.0%) were purchase from TCI. 2-Propanol (99.8%) and THF (99.6%) stabilized with BHT was purchased from Thermo Fischer Scientific. 4-Hydroxy-2,2,6,6-tetramethylpiperdinyloxyl (TEMPOL) and phenothiazine were provided by Hilti Entwicklungsgesellschaft mbH.

Synthetic procedures

Synthesis of bis-functional CTA. Bis-CDP was synthesized according to the reported procedure in the literature.[18]

Synthesis of betulin methacrylate (BetuMA). The procedure has been adapted from the one reported in the literature.[19] Transesterification was performed in a 1L-3-necked flask equipped with a magnetic stirrer, thermometer and a distillation apparatus. Heating was realized by an oil bath. 40 g of Betulin (90 mmol), 407 g of methyl methacrylate (MMA, 4.07 mol), 2.53 g of K_3PO_4 (12 mmol), 5.5 mg of TEMPOL (0.032 mmol) and 5.4 mg of phenothiazine (0.027 mmol) were mixed at room temperature. The reaction was considered to have started after the flask temperature reached *ca.* 70 °C and an azeotrope of MMA/MeOH was distilled off at around 350 mbar (abs.). The mixture was heated for total 17 h. After 6, 10, and 12 h, more K_3PO_4, respectively 0.7, 0.7 and 1.4 g were added. Samples were drawn during reaction to follow the hydroxyls conversion by ^{1}H-NMR spectroscopy. At the end, the mixture was filtrated to remove the insoluble salts, and MMA was distilled off in vacuum (80 mbar) at 40 °C for about 6 h. About 44 g of a light brown powder was recovered, the product mixture contains about 82 mol% of Betu-MA and about 8 mol% of dimethacrylated betulin. The latter was removed by purification with crystallization in *n*-hexane as reported:[20] the mixture was charged in a round flask with hexane (2% w/v) and heated at 60 °C for about 30 min; after that, the brown solution was immediately filtered. The filtered solution was stored in freezer overnight and the precipitated white material was recovered by filtration and dried in vacuum oven at 35 °C for about 24 h. About 30 g of pure BetuMA were recovered (yield 66%).

Synthesis of carvacryl methacrylate (CaMA). Reaction was executed according to the procedure reported in the literature.[21] A 100 mL Schlenk flask was backfilled with nitrogen, and 19.4 mL of carvacrol (120 mmol) 0.31 g of 4-dimethylaminopyridine (2.5 mmol) and 20 mL of methacrylic anhydride (0.13 mol) were added. After about 63 h at 45 °C, the flask was removed from the bath and the reaction stopped by addition of about 50 mL of ethyl acetate. For the work-up procedure, the organic phase was washed with 6 × 100 mL of saturated sodium bicarbonate solution, 3 × 100 mL NaOH 1 M, 3 × 100 mL NaOH 0.5 M, 2 × 100 mL HCl 1 M and 100 mL of water. The organic phase was dried over magnesium sulphate and solvent evaporated. About 20 g of CaMA (yield 70%) were recovered.

Synthesis of ET13 Macro-CTA. A 100 mL round Schlenk flask was purged with nitrogen and the reaction solution made of 30 g of ET13 (0.11 mol, 500 eq.), 193 mg (0.220 mol, 1 eq.) of bis-CDP (0.22 mmol) and 19 mg (0.11 mmol) of AIBN in 32 mL of dry toluene was added. Solution was purged with nitrogen flow and heated in an oil bath at 80 °C. After 7 h, the solution was quenched with air and precipitated in methanol three times. The viscous yellowish polymer was vacuum dried, and 26 g (86%) of product were recovered.

RAFT polymerization of BetuMA. In a 10 mL round flask purged with nitrogen were added in sequence: a solution of monomer BetuMA (1.0 g, 2.0 mmol, 100 eq.), CDP (7.9 mg, 0.020 mmol, 1 eq.), 19.6 μL of AIBN (0.1 M in dioxane, 0.0020 mmol, 0.1 eq.), and 1,3,5-trimethylbenzene (54.5 μL,

0.4 mmol, internal standard) in 3 mL of dry dioxane. Solution was purged with nitrogen for 15 minutes, then heated at 80 °C. Aliquots of the mixture were taken at different times for the kinetic study carried out by ^{1}H NMR and GPC analyses. After 6 h, the reaction solution was precipitated in methanol. After filtration, 0.29 g (30%) of PBetuMA were recovered.

RAFT polymerization of CaMA. In a 10 mL round flask purged with nitrogen were added 1.0 g of CaMA (4.6 mmol, 100 eq.), 18 mg of CDP (0.046 mmol, 1 eq.) 3.8 mg of AIBN (0.023 mmol, 0.5 eq.) in 1.1 mL of dry toluene. The solution was purged with nitrogen for about 15 minutes, followed by heating at 80 °C. Samples were taken at different times for the kinetic study by ^{1}H NMR and GPC analyses. After 8 h the polymer was precipitated in methanol, filtered, and dried recovering 0.3 g of PCaMA.

ABA triblock synthesis. A 50 mL round Schlenk flask purged with nitrogen was charged with 3.0 g of macro-CTA (M_n 108 kg mol^{-1}, 1 eq.), 1.06 g (2.1 mmol, 75 eq.) of BetuMA and 0.14 mL (0.1 M in dioxane, 0.014 mmol, 0.5 eq.) of AIBN in 32 mL dry dioxane. The solution was purged with nitrogen for 20 minutes, followed by heating at 80 °C for 3 h. After precipitation of the ABA-copolymer in methanol twice, the product was dried under vacuum at 40 °C to recover 3.4 g (84%) of copolymer.

Characterization methods

NMR. NMR ^{1}H NMR (500.13 MHz) and ^{13}C NMR (125.75 MHz) spectra were recorded using a Bruker Avance III 500 NMR spectrometer. DMSO-d_6 ($\delta(^1H)$ = 2.50 ppm, $\delta(^{13}C)$ = 39.52 ppm) and $CDCl_3$ ($\delta(^1H)$ = 7.26 ppm, $\delta(^{13}C)$ = 77.16 ppm) were used as the solvent and internal standard.

GPC. GPC analyses were carried out using THF as solvent with a flow rate of 1 mL min^{-1} at 25 °C. The instrument set up was as follows: pump system HPLC-Pump 1100 (Agilent Technologies), column 2 PL MIXED-C (300 × 7.5 mm and 5 μm PSgel). We used as detectors LS, DAWN-HELEOS-II (Wyatt Technology); RI, Optilab T-rEX (Wyatt Technology), UV, VWD 1260 (Agilent Technologies) at 310 nm and viscometer, ViscoStar-III (Wyatt Technology). M_n and $Đ$ were calculated by instrument software using previously evaluated dn/dc values.

DSC. DSC analysis was carried out with a Q2000 (TA Instruments, New Castle, DE, USA) in a temperature range of −100 to 150/250/325 °C at a scan rate of 10 K min^{-1} using nitrogen as purge gas. The T_g was determined from the second heating.

TGA. TGA analysis was carried out with a Q5000 (TA Instruments, New Castle, DE, USA) with a heating rate of 10 K min^{-1} in the temperature range of 20–800 °C with nitrogen as purge gas.

AFM. AFM measurements were done in the tapping mode by a Dimension ICON (Bruker-Nano, USA). We used OTESPA cantilevers (OPUS by MikroMasch) with nominal spring constants of 26 N m^{-1} and resonance frequencies of *ca.* 300 kHz. The nominal tip radius is lower than 7 nm. All measurements were performed consecutively with the same type of tip and scan rate of 1 Hz. Every image has a resolution of 512 px. The obtained data were processed by NanoScope Analysis 3.0 (Bruker, USA) and Gwyddion for determination of the domain sizes. For the latter, we first selected an appropriate threshold phase value (Table S2†) and used the grain analysis function to determine the mean grain size.

AFM sample preparation. The ABA triblock copolymers were dissolved overnight (13–19 mg in 1 mL dry THF) and filtered over 0.45 μm nylon syringe filter. Silica wafers, dimensions 1 × 2 cm, were cleaned in 2-propanol and THF, each for 15 minutes in ultrasonic bath, and followed by 20 minutes in the UV Ozone cleaner. 80 μl of the polymer solution were spin coated onto the silica wafer at 2000 rpm for 60 s.

WAXS. WAXS analysis was performed under ambient conditions in transmission mode, employing a D8 Discover X-ray diffractometer (Bruker, Billerica, MA, USA), equipped with a Vantec 500 area detector, and using CuKα radiation. The diameter of the circular beam was 0.5 mm, and the exposure time was 300 s. The sample-to-detector distance was 149.7 mm.

Results and discussion

The ABA triblock copolymers were synthesized *via* RAFT polymerization by a two-step procedure, as shown in Scheme 1. In the first step, the B block was obtained through RAFT polymerization using an "R-linked" bifunctional chain transfer agent (bis-CTA). The bifunctional macro-CTA was then employed in the second step for a RAFT chain extension of the termini.

The bis-CTA has been synthesized by esterification of the monofunctional CTA *S*-4-cyano-4-(dodecylthiocarbono thioylthio)pentanoic acid (CDP), reported to be a suitable CTA for methacrylates.[22]

Since the macro-CTA would represent the B block of the ABA structure, meaning the elastomeric part of the material, VISIOMER Terra C13-MA (ET13) has been chosen as monomer. Indeed, ET13 is a mixture of methacrylate alcohols having an average of C13 and thus it was considered suitable to provide polymers with low T_g. In the second step, the chain extension of the macro-CTA has been carried out with either BetuMA or CaMA. Such terpenes would confer rigidity to the B blocks, with the consequent formation of "hard" domains.

Overall, the study reported is organized as follow: preliminary investigations were conducted on the RAFT of terpene methacrylates BetuMA and CaMA, and on ET13 to determine the conditions of the process to control the chain growth at both low and high molecular weights. The best experimental conditions, in term of yield and kinetic control over the monomer conversion, have been employed in the second step for the synthesis of the final ABA structure.

RAFT polymerization of terpene methacrylates

The biobased compounds used for monomer synthesis were procured with high purity, first converted into methacrylates and purified before use – CaMA by washing and BetuMA by recrystallization. Only the soft block monomer ET13 (contain-

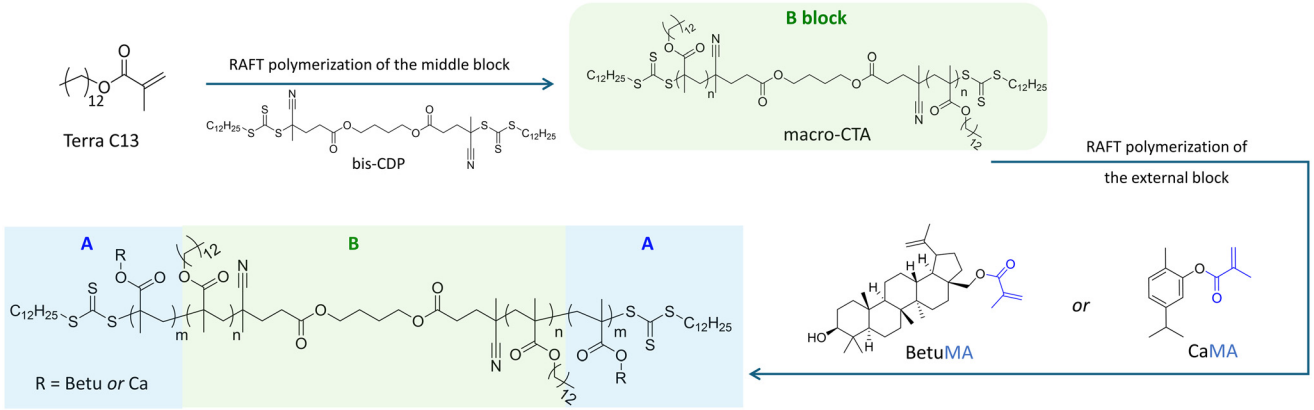

Scheme 1 Synthetic pathway of the ABA triblock.

ing ~5% MMA) was used without further procedure and according to NMR analysis there were no impurities (Fig. S3, S4, and S10†) to impair the radical polymerization.

Betulin, an abundant natural triterpenoid, presents three potential reactive sites: two hydroxyl groups (a primary and a secondary one) and an alkenyl group. The primary alcohol was selectively functionalized by a transesterification reaction to insert the polymerizable methacrylic group and form BetuMA (further details in ESI, Fig. S1–S3†). RAFT polymerization of BetuMA was carried out using CDP as the monofunctional CTA (Scheme 2). Results are reported in Table 1.

BetuMA was reported to be slightly soluble in toluene[20] thus, a polymerization was first conducted in such a solvent. However, despite using a large excess of toluene, precipitation occurred during the reaction (entry 1). Since dioxane was found to be a more appropriate solvent for both the monomer and polymer, the following polymerizations were performed in dioxane. CTA/initiator ratio was also adjusted to achieve a good conversion in a reasonable time. Albeit with a ratio CTA/AIBN = 2 or 5 an almost full conversion was reached in about 2 or 4 h (entries 2 and 3, respectively), increasing the ratio to 10 (entry 4), a pseudo first kinetic order (Fig. 1A, triangles) and a linear growth of the molecular masses (Fig. 1B, triangles) evidenced a better control over the process. Nevertheless, deviations from ideal RAFT behaviour were observed, such as an induction period and a final number-average molecular weight (M_n = 58.8 kg mol^{-1}), determined by GPC, that exceeded the theoretical value (M_n(th) = 46 kg mol^{-1}). Furthermore, the dispersity ($Đ$ = 1.4–1.7) remained higher than expected for a well-controlled system. These deviations may arise from non-ideal initiation associated with an incomplete CTA consumption.[23]

In conclusion, at 80 °C and with a CTA/AIBN ratio of 10, BetuMA exhibited a good polymerization kinetic, achieving nearly a complete conversion within 6 h. Besides, ^{1}H-NMR spectroscopy confirmed that the alkenyl group remained

Table 1 RAFT homo-polymerization of betulin methacrylate (BetuMA)

Entry	Solvent	T (°C)	CTA/AIBN ratio	t (h)	Conversion[a] (%)
1	Toluene[b]	80	2	8	>40[c]
2	Dioxane	80	2	2	94
3	Dioxane	80	5	4	97[d]
4	Dioxane	80	10	6	89[d]

Reaction conditions: molar equivalent BetuMA/CTA/AIBN 100/1/0.5, 0.2 or 0.1 in dioxane (76 wt%). [a] Determined by ^{1}H-NMR ($CDCl_3$) of the crude reaction mixture. [b] Toluene 90 wt%. [c] Polymer only partially soluble in toluene. [d] Determined using mesitylene as internal standard.

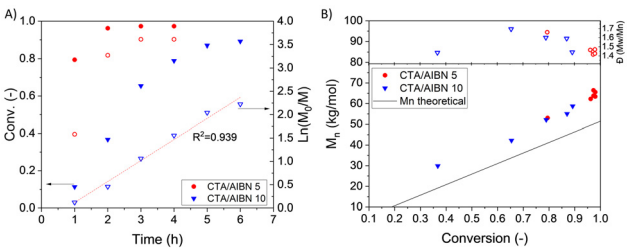

Fig. 1 RAFT polymerization of BetuMA: kinetic plot (A) and graph of M_n and $Đ$ *versus* monomer conversion (B) of entry 3 (circle) and entry 4 (triangle) of Table 1.

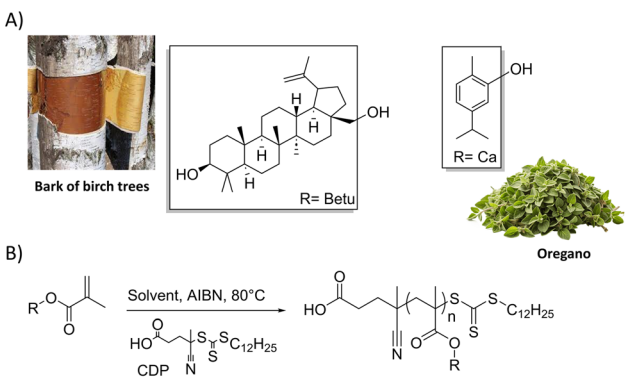

Scheme 2 (A) Betulin and carvacrol chemical structures and origins; (B) RAFT polymerization of betulin methacrylate (BetuMA) and carvacryl methacrylate (CaMA).

unreactive during the polymerization, indicating the high selectivity of RAFT for the methacrylic group. Contrarywise, when a free radical polymerization was performed in similar conditions (BetuMA 100 equiv., AIBN 0.2 equiv., Dioxane, 80 °C, 1 h), the formation of an insoluble microgel was observed.

RAFT polymerization of carvacryl methacrylate (CaMA) (Scheme 2) was carried out using CDP as monofunctional CTA and different targeted degrees of polymerization (DP_{target}). As reported in Table 2, good conversions were obtained at lower DP targets (entries 1 and 2), with kinetic plots showing a first order kinetics (Fig. 2A). GPC analyses confirmed a linear molecular mass growth, close to the theoretical one, and a quite good polydispersity index ($Đ < 1.3$) (Fig. 2B).

Both PBetuMA and PCaMA were characterized by TGA and DSC analyses (Fig. 3). PBetuMA exhibited outstanding thermal stability with a starting point of degradation above 300 °C, while PCaMA degradation began at around 160 °C, with the maximum loss at around 290 °C (Fig. 3A). DSC calorimetry evidenced a glass transition temperature (T_g) of about 79 °C and 220 °C for PCaMA and PBetuMA, respectively (Fig. 3B).

Finally, a kinetic study was carried out on the RAFT polymerization of ET13 with two different degrees of polymerization: DP 500 or DP 1500. In both cases, a first order kinetics, a linear growth of molecular masses *vs.* monomer conversion and low dispersities were observed, as shown in Fig. 4 (further details in ESI, Fig. S11–S14†).

Table 2 RAFT homo-polymerization of carvacryl methacrylate (CaMA)

Entry	DP_{target}	t (h)	Conversion (%)[a]	M_n (kg mol^{-1})[b]	$Đ$[b]
1	100	8	89	19.8	1.25
2	200	20	82	33.5	1.28
3	300	15	62	33.5	1.31

Reaction conditions: molar equivalent CaMA/CTA/AIBN DP_{target}/1/0.5 in 50 wt% toluene, 80 °C. [a] Determined by ^{1}H-NMR on the crude of reaction mixture. [b] Determined by GPC analysis.

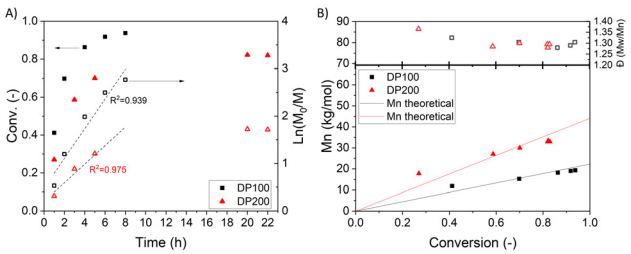

Fig. 2 RAFT polymerization of CaMA (A) kinetic plot and (B) M_n and $Đ$ *versus* conversion of entry 1 (square) and entry 2 (triangle) of Table 2.

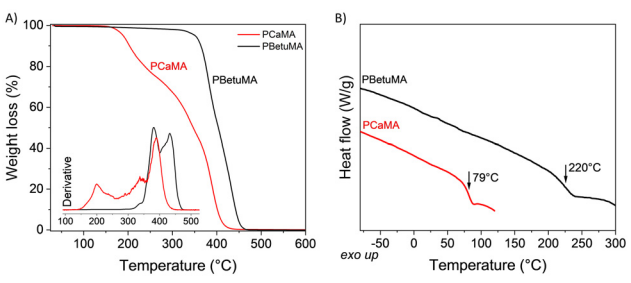

Fig. 3 Thermal analyses of BetuMA and CaMA homo-polymers (A) TGA curves and the relative derivative (inset) and (B) DSC second heating curve.

ABA triblock copolymers

ET13 bis-macro-CTA was synthesized by RAFT with an almost full conversion. Three macro-CTAs, named E1, E2 and E3, with M_n 84.1 kg mol^{-1}, 108 kg mol^{-1} and 229 kg mol^{-1}, respectively, have been then used for the following chain extension with BetuMA or CaMA (B and C, respectively in Table 3). Aiming to

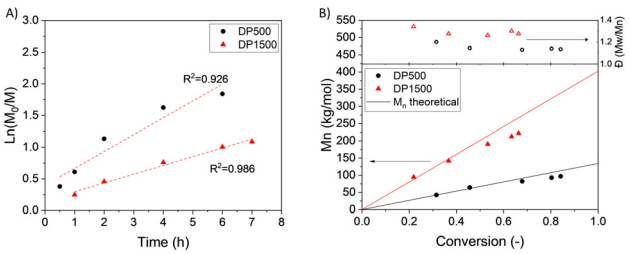

Fig. 4 RAFT polymerization of ET13 with two different degrees of polymerization (DP500 or DP1500): kinetic plot (A) and M_n and $Đ$ *versus* monomer conversion (B). Reaction conditions: ET13/bis-CTA/AIBN molar equivalent 500 or 1500/1/0.5 in 50 wt% toluene at 80 °C.

Table 3 Experimental conditions for the synthesis of ABA copolymers using E1, E2 or E3 as macro-CTAs, BetuMA (B) or CaMA (C) as monomers, and ABA structural characterization

ABA polymer	DP_{target}	Time (h)	Molar/weight fraction[a] (%)	M_n^{tot} (th)[b] (kg mol^{-1})	$M_n/Đ$[c] (kg mol^{-1})
BE_1B 1	50	3	8/14	97	105/1.12
BE_2B 2	80	3	10/17	122	127/1.21
BE_1B 3	100	5	17/28	116	138/1.17
BE_2B 4[d]	100	5	13/22	132	165/1.30
BE_3B 5[d]	200	1.5	9/17	275	207/1.55
BE_3B 6[d]	400	5	21/34	345	415/2.00
CE_1C 1	230	7	25/21	106	101/1.18
CE_1C 2	300	15	26/22	106	97/1.17
CE_1C 3	400	24	39/34	126	113/1.22
CE_3C 4	600	20	13/11	257	200/1.45
CE_3C 5	600	30	20/17	276	176/1.76

Macro-CTA: E1 (M_n = 84.1 kg mol^{-1}, $Đ$ = 1.10), E2 (M_n = 108 kg mol^{-1}, $Đ$ = 1.11), E3 (M_n = 229 kg mol^{-1}, $Đ$ = 1.25). Reaction conditions: BEB = macro-CTA/BetuMA/AIBN 1/DP_{target}/0.5 in dioxane (80 wt%) at 80 °C; CEC = macro-CTA/CaMA/AIBN 1/DP_{target}/0.5 in toluene (50 wt%) at 80 °C. [a] Relative glassy block amount determined by ^{1}H NMR spectroscopy (further details in Fig. S15†). [b] Total theoretical molecular weight: $M_n^{tot}(\text{th}) = M_n^E + \frac{DP_E \times X_B}{1 - X_B} \times MM_B$ where X_B and MM_B are the molar fraction and molecular mass respectively. [c] Determined by GPC in THF. [d] Toluene–dioxane mixture used as reaction solvent.

have ABA triblock copolymers with different fractions of the "hard" component, the reaction conditions have been changed using different monomer/macro-CTA ratios (meaning DP_{target}) or polymerization times. It is worth noting that generally in an ABA structure, TPEs are characterized by low amounts of the "hard" component; thus, the design of the final copolymer composition provided a percentage of BetuMA or CaMA in the range 15–30 wt%. Polymerization conditions and experimental results are reported in Table 3; the copolymer composition was estimated by ^{1}H NMR spectroscopy and representative spectra are reported in Fig. 5 (further details in ESI, Fig. S15–17†).

Triblock compositions (Table 3) spanned from 8 to 21 mol% for PBetuMA (BEB copolymers) and from 13 to 39 mol% for PCaMA (CEC copolymers). Since the macro-CTA with higher M_n, namely E3, was only partially soluble in dioxane, a mixture of toluene and dioxane was used as solvent (see BE_3B 5 and BE_3B 6 in Table 3) and for comparison purpose, BE_2B 4 was synthesized using the same solvent mixture.

Refractive index SEC chromatograms showed a time downshift of the copolymers' curves compared to that of the macro-CTA; moreover, all the final copolymers presented a narrow and monomodal dispersity clearly indicating the formation of copolymeric structures. Finally, the calculated absolute molecular weights were in good accordance with the theoretical ones (Fig. 6 and Fig. S18†). It should be noted that the extension of macro-CTA E3 appeared less effective than E1 or E2. Indeed, for the relative copolymers (CE_3C 4, CE_3C 5 and BE_3B 6) the chromatogram traces show tailing which increases with the hard block ratio, indicating a not ideal macro-CTA extension.

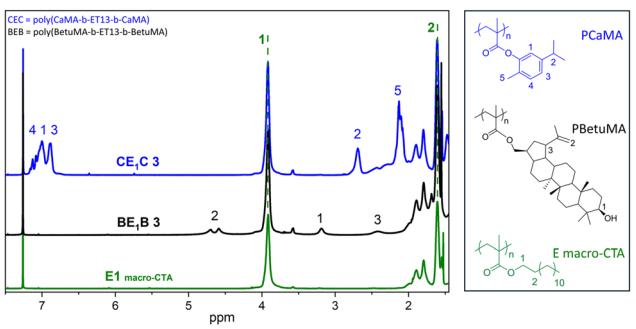

Fig. 5 Representative ^{1}H-NMR spectra of macro-CTA (E1) and the relative copolymers with BetuMA (BE_1B 3) or CaMA (CE_1C 3).

TPE characterization

Thermal properties. Thermal degradation of copolymers, as determined by TGA measurements, started at about 200 °C, similarly to ET13 macro-CTA (Fig. 7A), which was the predominant part of the ABA structure. It is worth noting that this temperature is also the degradation temperature of the RAFT terminal groups.[22] However, copolymers with higher amount of PBetuMA presented a retard of the second degradation step due to the higher thermal stability of PBetuMA blocks. For a phase separated block copolymer, two T_gs should be observed and indeed, in DSC analysis (Fig. 7B), CEC copolymers showed a lower T_g close to −50 °C and an upper one around 60 °C. For BEB samples, only one T_g was detected, specifically with a value close to that of the ET13 midblock, at around −50 °C. In DSC measurements up to 240 °C for different BEB polymers, the upper T_g was not detectable (second heating). Due to degradation of the midblock at these temperatures, the clear T_g determination was not possible. Since the presence of the block microstructure was previously confirmed by GPC measurements, the similarity of the T_g values between the BEB copolymers and the macro-CTA would be indicative of the blocks immiscibility and a microphase separation; besides, difficulties in determining the T_g associated to the minor component of block copolymers is often reported in literature.[24,25]

Morphological characterization. Analysis by atomic force microscopy (AFM) was carried out to further support the existence of a phase separation between the two blocks of the ABA copolymers. AFM in tapping-mode allowed imaging the surface morphology of selected films obtained by spin-coating, as well as material contrast between the different polymer phases. The observation of at least two regions with different AFM phase signals served as clear indication of the microphase separation.[26] In fact, the observed contrast in the phase images reflects the different viscoelastic response, among others, like adhesive properties and chemical interaction of the microphase domain with the oscillatory probe. Based on observation from studies on comparable systems, we can

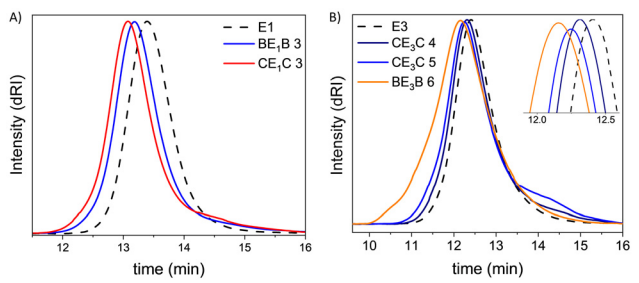

Fig. 6 Characteristic refractive index GPC traces of (A) macro-CTA E1 and of its relative copolymer and (B) macro-CTA E3 and its relative copolymer, with BetuMA (BEB) or CaMA (CEC).

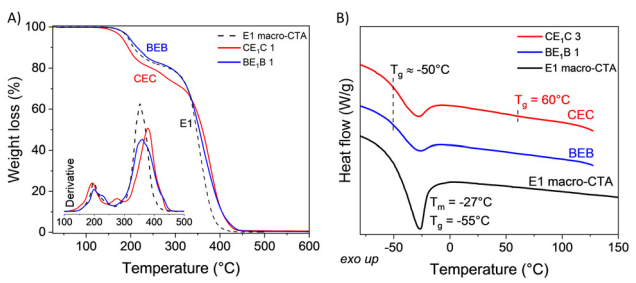

Fig. 7 (A) TGA scans and the relative derivative (inset), and (B) representative DSC second heating scans of E1 macro-CTA and its relative copolymers BEB and CEC.

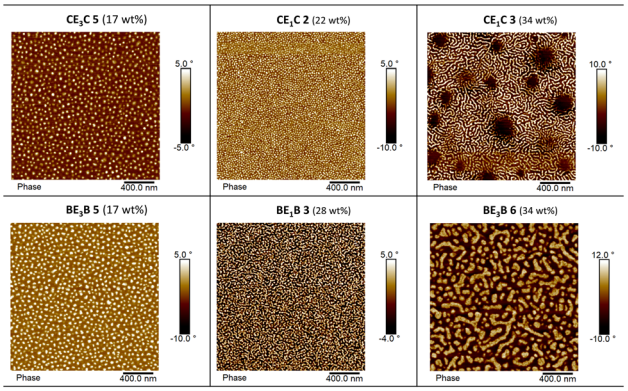

Fig. 8 AFM phase image of triblock copolymer with PCaMA (CE_3C 5, CE_1C 2 and CE_1C 3) or PBetuMA (BE_3B 5, BE_1B 3 and BE_3B 6) as external blocks. Corresponding topography images in ESI, Fig. S19.†

assume the zones with the brighter phase contrast relate to the stiffer blocks (external glassy blocks), and the darker zones to the softer block (middle block).[27] Fig. 8 shows the phase image of selected CEC and BEB copolymers. The film surface of the copolymer with 17 wt% and 22 wt% of PCaMA (CE_3C 5 and CE_1C 2), consisted of an assembly of small, hard domains (PCaMA) with spherical or cylindrical shape (average domain size CE_1C 2 = 18 nm, CE_3C 5 = 28 nm) in the soft block matrix phase. Increasing the PCaMA content to 34 wt% (CE_1C 3), the film surface showed bright elongated domains (38 nm) in a darker continuous matrix. This pattern can be interpreted as an interpenetrated assembly of the two blocks in a lamellar structure (Fig. 8).

Copolymers with PBetuMA at 17 wt% (BE_3B 5) presented an assembly of bright PBetuMA spheres (29 nm) in a dark PET13 matrix. As PBetuMA content increased (BE_2B 4 and BE_3B 6), samples exhibited a phase separation with a predominant lamellar structure. The domains of the two phases were larger for the sample with PBetuMA at 34 wt% (BE_3B 6 = 90 nm *vs.* BE_1B 3 = 30 nm).

Considering the significant difference in the structure of the two glassy block monomers, the morphological change is rather comparable with the different ratios. The low concentration of PBetuMA gives a very similar pattern to the low concentration of PCaMA, as do the medium and high concentrations. The difference is greatest for the latter, but the trend is clearly towards greater domain formation.

To investigate how the differences in the microdomain distribution translate into the mechanical properties of the polymer, the stress–strain behaviour was examined in the mechanical tests.

Mechanical testing. Stress–strain behaviour was determined by uniaxial tensile testing on dumbbell-shaped specimens cut from the polymer films. Transparent, light yellow (due to thiol group of the RAFT agent) and free-standing films (some tacky) were prepared from block copolymers by solvent casting. The average values obtained from at least three specimens are reported in Table 4, while Fig. 9 shows the corresponding stress–strain curves.

Table 4 Mechanical properties of ABA copolymers' film evaluated by tensile test

Sample	Glassy block, weight (%)	Modulus (MPa)	Ultimate strength, σ (MPa)	Elongation at break, ε (%)
BE_1B 1	14	0.43	1.1	524
BE_2B 2	17	0.17	0.7	532
BE_1B 3	28	132	6.2	238
BE_2B 4	22	8.0	3.9	363
BE_3B 5	17	0.32	1.4	759
BE_3B 6	34	11	3.9	359
CE_1C 1	21	0.24	1.0	526
CE_1C 2	22	0.22	0.8	428
CE_1C 3	34	1.7	1.2	274
CE_3C 4	11	0.07	0.2	437
CE_3C 5	17	0.14	0.7	710

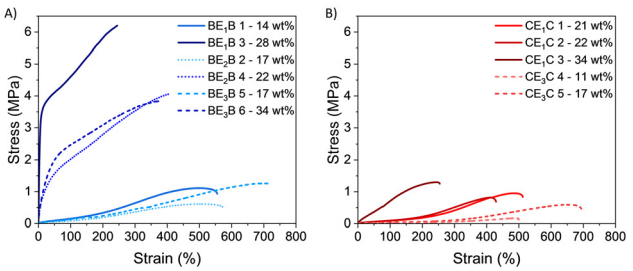

Fig. 9 Stress–strain graph of BEBs (A) and CECs copolymers (B) (solid lines indicates E1, dotted lines E2 and dashed lines E3 as macro-CTAs).

All samples show elastomeric behaviour with quasi linear stress–strain relationships and without any detectable yield point (Fig. 9).

An evident fast increase of initial modulus, which reached a remarkable final strength (σ) higher than 3 MPa and elongation at break (ε_b) between 240% and 360%, can be seen for samples containing more than 20% of PBetuMA, namely BE_1B 3, BE_2B 4 and BE_3B 6. Samples with a lower content of glassy blocks (BE_1B 1, BE_2B 2 and BE_3B 5) evidenced an elastomeric behaviour at low strain with a following hardening region, starting from about ε = 200%, typical of rubbers and TEPs (Fig. 9A). These samples exhibited a strength close to 1 MPa and an elongation at break ε_b above 500%. Noteworthy, the latter ε_b was higher when compared to the ε_b of samples with higher glassy amount.

Comparing copolymers with 17 wt% of PBetuMA but with different length of the middle block, the sample with the longest PET13 (BE_3B 5) presented higher elongation (ε_b = 760%) than the one with the shortest middle chain (BE_2B 2, ε_b = 530%). Looking at the tensile test results of CEC copolymers (Fig. 9B), all the samples analysed evidenced an elastomeric behaviour with strength close to or below 1 MPa and an elongation at break decreasing as PCaMA content increased. For example, CE_1C 3, containing the highest amount (34 wt%), exhibited a rapid increase of strength up to 1.2 MPa and the lowest ε_b = 270%. When comparing samples with similar

length of PET13 (E1 and E2), CECs copolymers showed slightly lower elongation ($\varepsilon_b \approx 420$–$500\%$) than BEB samples ($\varepsilon_b \approx 530\%$), but a comparable ultimate strength in the range 0.7–1.1 MPa.

Finally, all the samples with E3 as the middle block showed a different behaviour depending on the nature of the hard blocks; indeed, copolymers containing CaMA showed the lowest strength ($\sigma < 0.7$ MPa). This can be evidenced by comparing samples with 17 wt% of glassy block content: CE_3C 5 showed $\varepsilon_b = 710\%$ and $\sigma = 0.65$ MPa, while BE_3B 5 had $\varepsilon_b = 760\%$, and $\sigma = 1.35$ MPa (Table 4).

Generally, as the glassy content increased, the modulus and the ultimate tensile stress increased as well, while the elongation at break decreased; however, the magnitude of this behaviour depended on the nature of the glassy blocks. A comparison of elongation and strength *versus* the nature and the amount of the glassy component is reported in Fig. 10. By increasing the glassy content, copolymers with BetuMA (BEB) showed a more marked tensile strength increase (Fig. 10, upper panel, blue circle) compared to copolymers with CaMA (CEC) (Fig. 10, red circle). Finally, similar properties are feasible with far less molar percent of BetuMA compared to CaMA: for example, a tensile strength around 1 MPa and an elongation around 500% were shown by samples with 8–10 mol% of BetuMA (14–17 wt%), while similar properties are achievable with about 25–26 mol% of CaMA (21–22 wt%). The correlation of the mechanical characteristics with the glassy block behaviour depending on the monomer structure was further investigated with X-ray analysis to determine possible crystalline domains.

X-ray analysis. Wide-angle X-ray scattering WAXS was used to investigate the crystallinity of the bulk structure and was performed on the same film prepared for mechanical testing. Diffractograms of selected samples are shown in Fig. 11. They show three main reflexes at about 18.5° (d = 0.479 nm), 31° and 42°. These findings agree with previous reported data for poly(*n*-alkyl methacrylate).[13,28]

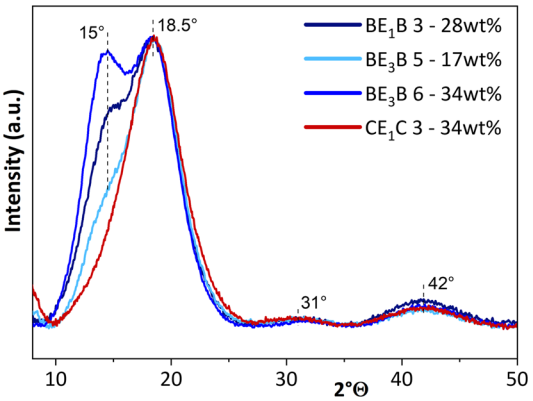

Fig. 11 WAXS diffractograms of selected ABA copolymers.

The peak with an equivalent Bragg spacing of about 0.5 nm corresponds to the van der Waals (VDW) contacts of atoms and is known as the VDW peak. Samples with PCaMA as external blocks, even at high content of CaMA (CE_1C 3, 34 wt%), show evidence only of reflexes associated with the middle block. On the other hand, samples containing PBetuMA showed a shoulder with a maximum at about 15° that became more evident as the PBetuMA content increased in the copolymer. This reflex could be due to a partial organization of the betulin rings in a stacked structure, forming crystalline domains. Indeed, betulin itself was reported to form crystalline structures with the more intense peak showing a maximum around 14–15°.[29] This finding supports the AFM results on the formation of larger hard block domains with increasing PBetuMa content (Fig. 8), which also impacts the stress–strain behaviour. Leading to the highest tensile strength, but the lowest strain and elongation values (Fig. 9 and 10).

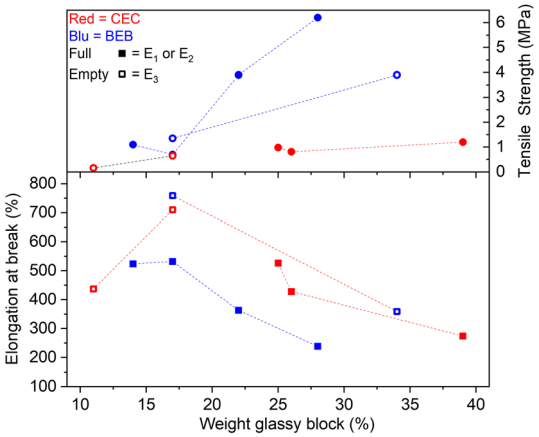

Fig. 10 Comparison of copolymers elongation (lower panel) and tensile strength (upper panel) *versus* glassy block (Red symbols represent CECs while blue ones BEBs; full symbols represent copolymers made with E1 or E2 as macroCTA, while empty symbols are for copolymers made by E3).

Conclusions

This study demonstrates the successful synthesis of biobased acrylic ABA triblock copolymers *via* RAFT polymerization, emphasizing the potential of renewable materials in thermoplastic elastomer (TPE) applications. The use of biobased monomers ET13, BetuMA, and CaMA resulted in ABA block copolymers with control of molar mass and a well-defined block structure.

Thermal analysis confirmed good stability and a well distinct phase separation, essential for TPE materials, was observed *via* AFM and supported by DSC and WAXS analysis. Tensile tests showed the presence of elastomeric behaviour for all the block copolymers, with better performance of BEBs compared to CECs. Furthermore, the BEB block copolymers, incorporating BetuMA, achieved high tensile strength and elongation at break with a lower glassy block content, reflecting the superior properties of BetuMA (high T_g = 220 °C, for-

mation of crystalline domains) compared to CaMA as hard block forming monomer and a different influence of the glassy block nature on the mechanical properties. BEB copolymers, particularly those with moderate glassy block content (*e.g.* BE_3B 5), provide an optimal combination of tensile strength and elongation at break. Higher glassy block content increases stiffness but sacrifices elongation. The macro-CTA molecular weight influences the elongation and strength significantly, with E3-based samples showing superior elongation.

Overall, BEB and CEC samples provide a competitive and sustainable alternative to similar oil-based triblock copolymers reported in the literature. Besides, BEBs have only slightly lower performance when compared to an all-acrylic commercial TPE (Kurarity LA2140e, poly(MMA-butyl acrylate-MMA), 23% MMA, σ = 8.1 MPa, ε = 580%).[24]

These findings underscore the viability of biobased TPEs as sustainable alternatives to fossil-derived counterparts, paving the way for further research into optimizing their performance and expanding their industrial applications.

Author contributions

A. V. investigation, data curation, validation, writing – original draft. P. S. conceptualization, supervision, investigation, writing – original draft. I. H. data curation, writing – review & editing. Q. L. AFM data acquisition and formal analysis. B. V. supervision, writing – review & editing. L. I. supervision, writing – review & editing, funding acquisition.

Conflicts of interest

There are no conflicts to declare.

Data availability

The data supporting this article have been included as part of the ESI.† All raw and *meta* data of the measurements are saved in the institute server and are available on request.

Acknowledgements

We want to thank our supporting colleagues at IPF, especially Regine Boldt, for the WAXS measurements and Hartmut Komber for the help with the NMR investigations. Also, we want to acknowledge Karsten Scheibe for the mechanical measurements on our delicate samples and Kerstin Arnhold for the TGA & DSC measurements. Evonik, we are grateful to for providing the free sample of VISIOMER® Terra C13. AV and LI are thankful for the support of ESF (European Social Fund) – REACTEU Programme (DM 1061/2021).

References

1 J. G. Drobny, in *Handbook of thermoplastic elastomers*, PDL (Plastics Design Library)/William Andrew Pub, Norwich, NY, 2014.
2 *Advances in thermoplastic elastomers: challenges and opportunities*, ed. N. K. Singha and S. C. Jana, Elsevier, Amsterdam London Cambridge, 2024.
3 J. H. Jeon, J. H. Jung and C. Choi, *J. Polym. Sci.*, 2023, **62**, 662.
4 A. Vittore, O. Santoro, M. Candida, S. Vaghi, S. Pragliola, M. Mella and L. Izzo, *Polymer*, 2025, **324**, 128228.
5 F. Molinari, A. Salini, A. Vittore, O. Santoro, L. Izzo, S. Fusco, L. Pollegioni and E. Rosini, *Bioresour. Technol.*, 2024, **408**, 131190.
6 K. Y. Cho, S. S. Hwang, H. G. Yoon and K.-Y. Baek, *J. Polym. Sci., Part A:Polym. Chem.*, 2013, **51**, 1924–1932.
7 S. Wang, W. Ding, G. Yang and M. L. Robertson, *Macromol. Chem. Phys.*, 2016, **217**, 292–303.
8 M. Nasiri, D. J. Saxon and T. M. Reineke, *Macromolecules*, 2018, **51**, 2456–2465.
9 K. Satoh, D. Lee, K. Nagai and M. Kamigaito, *Macromol. Rapid Commun.*, 2014, **35**, 161–167.
10 W. Ding, S. Wang, K. Yao, M. S. Ganewatta, C. Tang and M. L. Robertson, *ACS Sustainable Chem. Eng.*, 2017, **5**, 11470–11480.
11 C. Veith, F. Diot-Néant, S. A. Miller and F. Allais, *Polym. Chem.*, 2020, **11**, 7452–7470.
12 Y. Xia and R. C. Larock, *Green Chem.*, 2010, **12**, 1893–1909.
13 D. P. Chatterjee and B. M. Mandal, *Macromolecules*, 2006, **39**, 9192–9200.
14 F. Asempour, E. Laurent, Y. Ecochard and M. Maric, *ACS Appl. Polym. Mater.*, 2024, **6**, 956–966.
15 S. Tajbakhsh, F. Hajiali and M. Marić, *Ind. Eng. Chem. Res.*, 2020, **59**, 8921–8936.
16 N. Leyva-López, E. Gutiérrez-Grijalva, G. Vazquez-Olivo and J. Heredia, *Molecules*, 2017, **22**, 989.
17 S. A. Kuznetsova, G. P. Skvortsova, I. N. Maliar, E. S. Skurydina and O. F. Veselova, *Russ. J. Bioorg. Chem.*, 2014, **40**, 742–747.
18 T. M. Hinton, C. Guerrero-Sanchez, J. E. Graham, T. Le, B. W. Muir, S. Shi, M. L. V. Tizard, P. A. Gunatillake, K. M. McLean and S. H. Thang, *Biomaterials*, 2012, **33**, 7631–7642.
19 P. Voigt, N. Kiriy, K. Jähnichen and B. Voit, *ACS Sustainable Chem. Eng.*, 2024, **12**, 1984–1996.
20 D. V. Orekhov, A.P. Sivokhin, A. S. Simagin, O. A. Kazantsev, K. V. Otopkova, A. D. Ovchinnikov, I. N. Makhov and N. B. Melnikova, *Polym. Adv. Technol.*, 2023, **34**, 2529–2540.
21 J. F. Stanzione, J. M. Sadler, J. J. La Scala and R. P. Wool, *ChemSusChem*, 2012, **5**, 1291–1297.
22 *RAFT Polymerization*, ed. G. Moad and E. Rizzardo, Wiley, 1st edn, 2021, vol. 1.

23 S. Boner, K. Parkatzidis, N. D. A. Watuthanthrige and A. Anastasaki, *Eur. Polym. J.*, 2024, **205**, 112721.
24 S. Wang, L. Shuai, B. Saha, D. G. Vlachos and T. H. Epps, *ACS Cent. Sci.*, 2018, **4**, 701–708.
25 J. J. Gallagher, M. A. Hillmyer and T. M. Reineke, *ACS Sustainable Chem. Eng.*, 2016, **4**, 3379–3387.
26 A. Rasmont, P. Leclère, C. Doneux, G. Lambin, J. D. Tong, R. Jérôme, J. L. Brédas and R. Lazzaroni, *Colloids Surf., B*, 2000, **19**, 381–395.
27 W. Wang, R. Schlegel, B. T. White, K. Williams, D. Voyloy, C. A. Steren, A. Goodwin, E. B. Coughlin, S. Gido, M. Beiner, K. Hong, N.-G. Kang and J. Mays, *Macromolecules*, 2016, **49**(7), 2646–2655.
28 G. Floudas and P. Štepánek, *Macromolecules*, 1998, **31**, 6951–6957.
29 X. Niu, E. J. Foster, B. O. Patrick and O. J. Rojas, *Adv. Funct. Mater.*, 2022, **32**, 2206058.